Received 6 March 2009
Revised 6 July 2009
Accepted 17 July 2009

Biomagnetic fluid flow in the presence of a line dipole

Polycarpos K. Papadopoulos
Department of Engineering Sciences, University of Patras, Patras, Greece

Abstract

Purpose – The purpose of this paper is to investigate the effect of a magnetic field on the flow of a biomagnetic fluid.

Design/methodology/approach – The flow takes place in a straight circular duct and the magnetic field is produced by a line dipole placed perpendicularly to the longitudinal axis of the duct.

Findings – The numerical results show that the magnetic field affects the characteristics of the flow, the velocity components and the friction factor, even for medium field intensity. A relation is proposed for the maximum and minimum longitudinal pressure drop in the pipe.

Originality/value – From the present results it is obtained that it is important to take into account the magnetic properties of blood in the various applications that involve blood flow in the presence of a magnetic field.

Keywords Blood, Magnetic fields, Laminar flow, Biotechnology

Paper type Research paper

1. Introduction

The use of magnetorheological biofluids for medical purposes is a very promising technique in medicine. Their magnetic properties can be utilized in cancer therapy in order to mechanically block blood vessels that nourish the tumor (Liu *et al.*, 2001) or in applications of blood detoxification and in techniques devised for the extraction of magnetic particles from the blood stream (Kaminski and Rosengart, 2005; Mykhaylyk *et al.*, 2005; Ganguly *et al.*, 2005a, b; Ganguly and Puri, 2007). The design of such techniques requires good knowledge of the behavior of the biomagnetic fluid and the forces that arise when a magnetic field is applied. In that case, the magnetic properties of the biomagnetic fluid play an important role and their effect on the flow should be taken into account.

Towards this aim, in the last few years, several studies have dealt with the issue of biomagnetic fluid dynamics (BFD) (Roath, 1993; Ruuge and Rusetski, 1993). A biomagnetic fluid is a fluid that exists in a living creature and its flow is influenced by the presence of a magnetic field. The most common biomagnetic fluid is blood and its magnetic properties are due to the hemoglobin that is contained in the erythrocytes. The study of the magnetic anisotropy of blood cells has shown that the level of oxygenation of the hemoglobin molecule alters the magnetic properties of erythrocytes from diamagnetic (oxygenated state) to paramagnetic (deoxygenated state) (Higashi *et al.*, 1993; Sakhini, 2003; Shalygin *et al.*, 1983; Takeuchi *et al.*, 1995; Higashi *et al.*, 1997).

For the investigation of BFD, Haik *et al.* (1999, 2001) and Motta *et al.* (1998) proposed a model which was based on the principals of ferrohydrodynamics (FHD) and considered biomagnetic fluids as homogeneous, Newtonian fluids affected by spatially varying magnetic fields. Tzirtzilakis (2005), Papadopoulos and Tzirtzilakis (2004) and Tzirtzilakis and Loukopoulos (2005) extended this model by taking into account the principles of magnetohydrodynamics and showed that the effect of the electrical conductivity of the biofluid is significant in cases of uniform magnetic fields.

In the present study we investigate the developing flow of a biomagnetic fluid in a straight circular duct which has a magnetic line dipole placed perpendicularly to its

International Journal of Numerical Methods for Heat & Fluid Flow
Vol. 20 No. 3, 2010
pp. 298-311

0961-5539
DOI 10.1108/09615531011024057

longitudinal axis. The geometry that we consider is a circular tube flow configuration that is very similar to real blood vessels or external ducts used in blood-related applications. The spatially varying magnetic field affects the flow behavior, the share stresses and the friction factor of the flow, which play a critical role in diseases such as atherosclerosis and thrombosis (Taylor and Humphrey, 2009). In the present investigation we consider several values of the parametric magnetic number *Mn* which depends mainly on the diameter of the duct (biomagnetic fluid vessel), the intensity of the magnetic field and the susceptibility of the biofluid. The investigation yields to useful results that can be utilized in various technological applications related to hemodynamics, such as magnetic drug targeting, hyperthermia cancer treatment and blood detoxification.

The magnetic properties of blood are important in applications which involve strong and medium magnetic fields. Thus, the present study is not restricted to strong magnetic fields of the order of 10 T which can be produced only by magnetic resonance imaging techniques. It is found that even for medium intensity fields, with induction of the order of 0.5 T, there is a local variation of the friction coefficient of up to 10 per cent. This information is crucial to the modeling of the behavior of drug carrying ferrofluids in the human body under the effect of magnetizable implants or external magnetic fields (Mathieu *et al.*, 2006; Rotariu and Strachan, 2005; Voltairas *et al.*, 2002; Rosengart *et al.*, 2005). The quantification of the biomagnetic flow characteristics could aid to the understanding of BFD and to the improvement of disease treating techniques.

2. Analysis

We consider the problem of laminar incompressible flow of a homogeneous, Newtonian, biomagnetic fluid through a straight circular pipe. Beneath the pipe there is a line dipole as shown in Figure 1, which generates a magnetic field. The dipole is placed in the x-direction at $d_a = D/50$ below the duct, with D the diameter of the duct. The contours of the spatially varying magnetic field strength are shown in Figure 1a. The magnetic field inside the biomagnetic fluid can be represented by:

$$\mathbf{B} = \mu_0(1+\chi)m\left(\frac{\sin\varphi}{r^2}\mathbf{e}_r - \frac{\cos\varphi}{r^2}\mathbf{e}_\varphi\right) \tag{1}$$

where μ_0 is the magnetic permeability of vacuum, χ is the magnetic susceptibility of the biofluid, $m \equiv Ib/(2\pi)$ for electrical current I and dipole wire distance b and r is the distance from the centerline of the coil, which is considered as the virtual line origin of the dipole, extending in the x-direction. Equation (1) shows that the magnetic field induction $\mathbf{B}$ decreases very rapidly with the distance from the dipole, at a rate proportional to the inverse square of this distance. Thus, the field affects the fluid only in the vicinity of the line dipole, which is the area that must be treated, and leaves the rest of the flow unaffected. The orientation of the resulting magnetic field is shown in Figure 1.

The Maxwell equations that describe the magnetic field are:

$$\nabla \times \mathbf{H} = 0 \tag{2}$$

$$\nabla \cdot \mathbf{B} = 0 \tag{3}$$

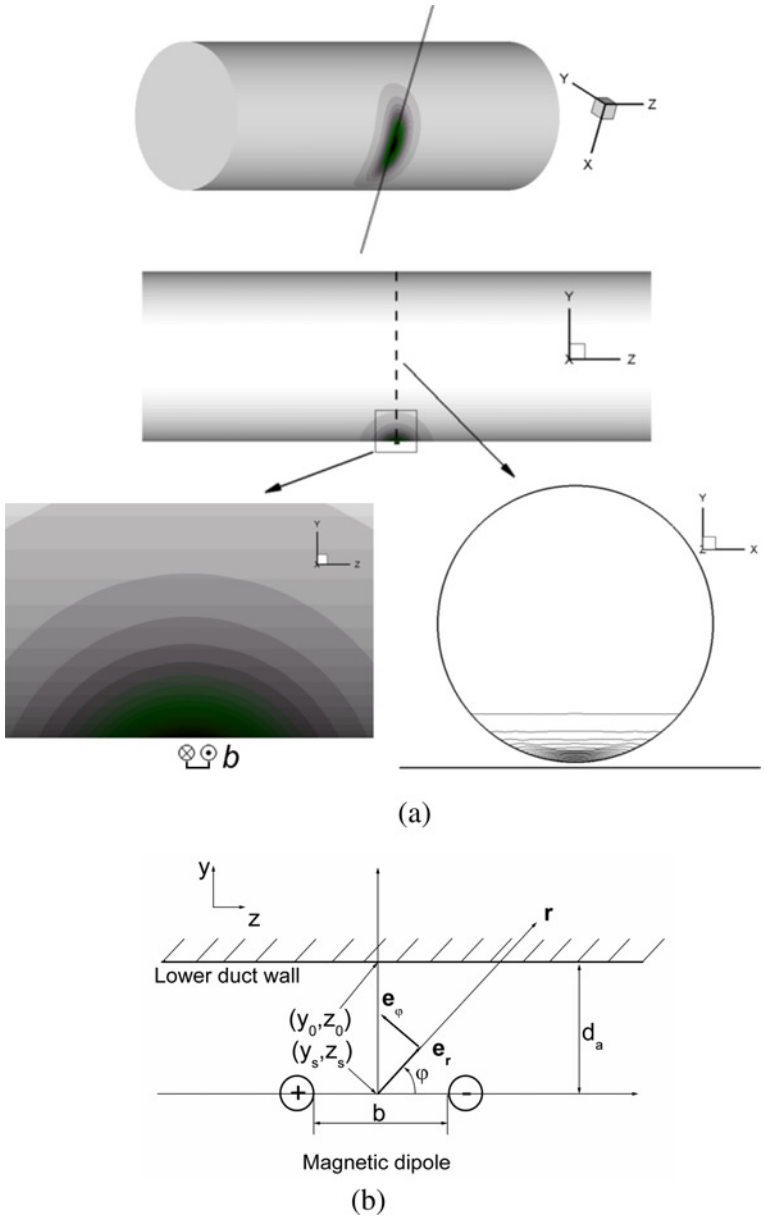

Figure 1.
Configuration of the duct, coordinate system and magnetic field

where **H** is the magnetic field strength. For the magnetization **M**, we use the following linear equation which is valid for isothermal cases:

$$\mathbf{M} = \chi \mathbf{H} \tag{4}$$

The governing equations are the continuity equation and the momentum equation:

$$\nabla \mathbf{V} = 0 \tag{5}$$

$$(\mathbf{V}\nabla)\mathbf{V} = -\frac{1}{\rho}\nabla P + \nu\nabla^2\mathbf{V} + \frac{\mu_0}{\rho}(\mathbf{M}\nabla)\mathbf{H} \tag{6}$$

where ρ is the density and ν is the kinematic viscosity. These equations conform to the BFD model (Haik *et al.*, 2001; Motta *et al.*, 1998) which is consistent with the principles of FHD. The Lorentz force due to the electrical conductivity of the biofluid (blood) is negligible due to the orientation of the magnetic field.

The dimensionless variables used for the transformation of the governing equations are:

$$\begin{aligned} &x, y, z = (X, Y, Z)/D, \quad u, v, w = (U, V, W)D/\nu \\ &p = PD^2/\rho\nu^2 \quad H = \frac{H_{\text{dimensional}}}{H_0} \end{aligned} \tag{7}$$

where H_0 is the magnitude of the magnetic field strength at point (y_0, z_0) (Figure 1b).

For the computations we used a boundary fitted coordinate system, generated numerically through the solution of a system of elliptic equations. This technique was developed by Thompson *et al.* (1974) and has been applied to various problems involving irregular geometries such as airfoils and nozzles. The orthogonality of the grid on the boundaries is achieved by a grid point control technique proposed by Thomas and Middlecoff (1980). Thus, the governing equations are transformed from the Cartesian system (*x, y, z*) to a boundary fitted coordinate system (ξ, η, *z*) as shown in Figure 2. The equations are then expressed in the non-dimensional variables defined above, in the parabolic formulation which is suitable for developing flows. The longitudinal direction is along the *z*-axis and *w* is the corresponding velocity component. The governing equations become

Continuity equation:

$$\frac{\partial \bar{U}}{\partial \xi} + \frac{\partial \bar{V}}{\partial \eta} + J\frac{\partial w}{\partial z} = 0 \tag{8}$$

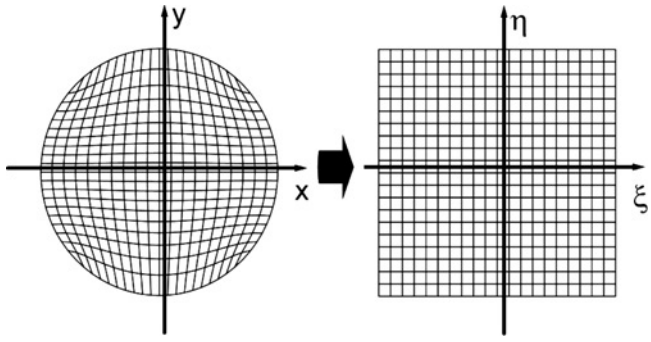

Figure 2.
Transformation to the boundary fitted coordinate system

u-momentum equation:

$$\frac{\partial(\bar{U}u)}{\partial\xi}+\frac{\partial(\bar{V}u)}{\partial\eta}+J\frac{\partial(wu)}{\partial z}=-\left(\frac{\partial p}{\partial\xi}y_\eta-\frac{\partial p}{\partial\eta}y_\xi\right)+\frac{1}{J}\left(\alpha\frac{\partial^2 u}{\partial\xi^2}-2\beta\frac{\partial^2 u}{\partial\xi\partial\eta}+\gamma\frac{\partial^2 u}{\partial\eta^2}\right) \tag{9}$$

v-momentum equation:

$$\frac{\partial(\bar{U}v)}{\partial\xi}+\frac{\partial(\bar{V}v)}{\partial\eta}+J\frac{\partial(wv)}{\partial z}=\left(\frac{\partial p}{\partial\xi}x_\eta-\frac{\partial p}{\partial\eta}x_\xi\right)+\frac{1}{J}\left(\alpha\frac{\partial^2 v}{\partial\xi^2}-2\beta\frac{\partial^2 v}{\partial\xi\partial\eta}+\gamma\frac{\partial^2 v}{\partial\eta^2}\right)+MnH\left(-\frac{\partial H}{\partial\xi}x_\eta+\frac{\partial H}{\partial\eta}x_\xi\right) \tag{10}$$

w-momentum equation:

$$\frac{\partial(\bar{U}w)}{\partial\xi}+\frac{\partial(\bar{V}w)}{\partial\eta}+J\frac{\partial(w^2)}{\partial z}=-J\frac{dp_a}{dz}+\frac{1}{J}\left(\alpha\frac{\partial^2 w}{\partial\xi^2}-2\beta\frac{\partial^2 w}{\partial\xi\partial\eta}+\gamma\frac{\partial^2 w}{\partial\eta^2}\right)+JMnH\frac{\partial H}{\partial z} \tag{11}$$

where $\bar{U},\bar{V}$ are the contravariant velocity components and Mn is the dimensionless magnetic number. These quantities along with the Jacobian and the transformation coefficients α,β,γ are defined in the following relations:

$$\begin{aligned}&\bar{U}=uy_\eta-vx_\eta,\quad \bar{V}=vx_\xi-uy_\xi,\quad Mn=\frac{\mu_0\chi D^2H_0^2}{\nu^2\rho}\\&J=x_\xi y_\eta-x_\eta y_\xi,\quad \alpha=x_\eta^2+y_\eta^2,\quad \beta=x_\xi x_\eta+y_\xi y_\eta,\quad \gamma=x_\xi^2+y_\xi^2\end{aligned} \tag{12}$$

At the boundaries of the duct we impose the no-slip boundary condition. As initial condition we consider a fully developed flow in a straight duct. The inlet of the duct is taken far upstream from the magnetic dipole where the effect of the magnetic field is negligible.

The mean axial velocity, which in the present non-dimensional form coincides with Reynolds number, is given by:

$$\mathrm{Re}\equiv\bar{w}=\frac{\int_A w dA}{\int_A dA} \tag{13}$$

Two quantities of great interest are the friction factor product with the Reynolds number, fRe and the friction coefficient product with Re, C_fRe. These quantities are given by the relations:

$$f\,\mathrm{Re}=-2\frac{dp_a/dz}{\bar{w}}\quad\text{and}\quad C_f\,\mathrm{Re}=2\frac{\tau_s}{\bar{w}} \tag{14}$$

where τ_s is the shear stress at the wall of the duct.

3. Numerical implementation

The governing equations were solved according to the closest vector problem (CVP) algorithm (Hatzikonstantinou and Sakalis, 2004; Sakalis *et al.*, 2005) with the use of a chlorinated polyvinyl chloride grid (Papadopoulos and Hatzikonstantinou, 2004). The technique used for treating the parabolic flow was similar to the one employed by Patankal and Spalding (1972) and it was a marching in the axial direction algorithm based on the mass flow rate conservation. The details of the method can be found in Papadopoulos *et al.* (2008). The convection and diffusion terms were discretized with the second-order central differences scheme except from the first-order axial derivatives where we used second-order backward differences.

The criterion for convergence at each axial step was:

$$\frac{1}{N}\sum_{i=2}^{i_{\max}-1}\sum_{j=2}^{j_{\max}-1}\left|\frac{\Phi_{i,j}^{n+1}-\Phi_{i,j}^{n}}{\Phi_{i,j}^{n+1}}\right| \leq 10^{-5} \tag{15}$$

where $\Phi \equiv u, v, w$, the total number of grid points is N and the subscripts i, j represent the nodes of the ξ, η coordinates, respectively.

The computations were conducted on a mesh of 48×48 cells in the transversal plane and in order to predict accurately the axial flow, the axial step was chosen to be $\Delta z = \Delta\xi/3 = \Delta\eta/3$. Thus, for a duct of dimensionless diameter of $d = 1$ and of axial length $z = 5$, the mesh had a size of approximately $48 \times 48 \times 720$ cells. We also ran test cases with a coarser mesh of 30×30 cells in the transversal plane and the difference in the value of the predicted axial pressure gradient, with the present 48×48 grid was found to be 3.5 per cent. For a finer grid of 60×60, the difference with the present 48×48 mesh was less than 1 per cent. Thus, with the present grid, we combined independence of the results from the mesh size and computational efficiency.

In order to assure the accuracy of the predictions of the present method, computations were conducting for flow in a curved circular pipe and the results were compared to the experimental data of Bovendeerd *et al.* (1987) for flow in a circular 90° curved tube. The CVP method was applied on a $48 \times 48 \times 180$ grid. The flow corresponds to $\mathrm{Re} = 700$ in a pipe with dimensionless curvature 1/3 and the results correspond to downstream angles 4.5°, 11.5°, 23.5°, 40°, 58.5° and 82°. The plots of Figure 3 show the distribution of the normalized axial velocity $w/\bar{w}$ along the horizontal ξ-axis. The CVP results are in very good agreement with the experimental data.

Another comparison was made with the results of Ganguly *et al.* (2005a-c) and Ganguly and Puri (2007) who examined numerically and experimentally, ferrofluid flow in a channel under the influence of a magnetic field. The flow behavior predicted in the present study is in excellent agreement with the numerical results of Ganguly *et al.* (2005c) for ferrofluid flow over a magnetic dipole. The fluid is repelled by the magnetic field in the area above the magnetic dipole and the axial velocity presents wave-like formations. Moreover, the obstacle-like effect of the magnetic field in the flow is observed in the experimental and numerical investigation (Ganguly *et al.*, 2005a).

4. Results and discussion

In order to obtain a connection between the dimensionless computational results and the physical quantities encountered in real applications, we examine the following flow case. For flow in a large vessel with circular cross-section [$D = 0.012$ m], with deoxygenated blood as the working medium [$\rho = 1{,}050\,\mathrm{kg/m^3}$, $\nu = 3.1 \times 10^{-6}\,\mathrm{m^2/s}$,

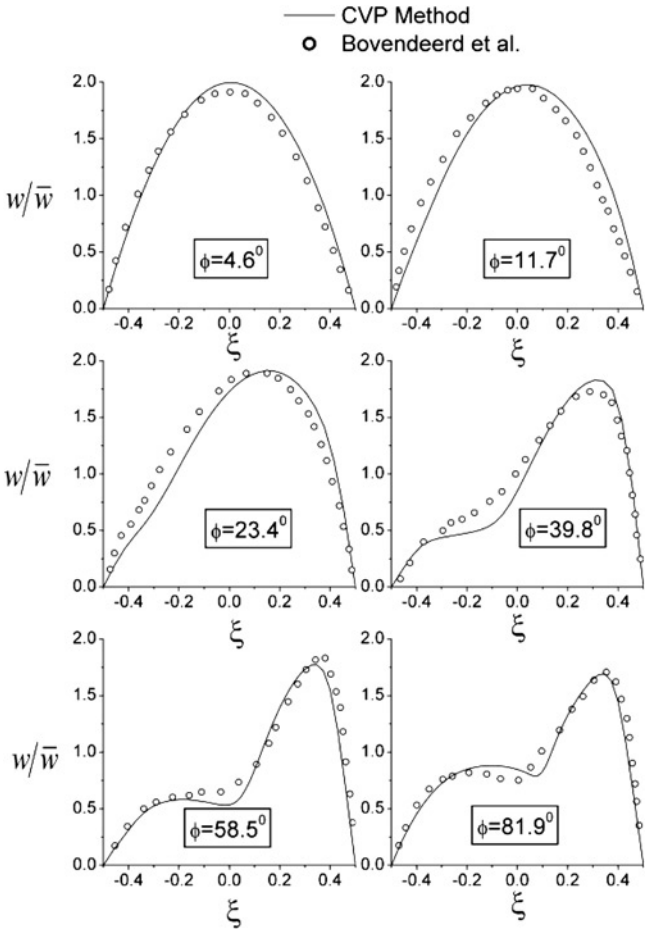

Figure 3.
Comparison between the present numerical results for the axial velocity development and experimental data of Bovendeerd *et al.* (1987) for flow with Re = 700 in a pipe with dimensionless curvature 1/3

$\chi = 3.5 \times 10^{-6}$] with $\mu_0 = 4\pi \times 10^{-7}$ mkg/A^{2}s^2, the magnetic number $Mn = 10^4$ corresponds to a field induction of $B = 0.5$ T. This can be achieved by placing a dipole whose wires have a distance of $b = 0.05$ m between them at a distance of $d_a = 0.6$ mm from the vessel, and apply electrical current of $I = 20$ A, according to Equation (1). This hypothetical case demonstrates the practical significance of the dimensionless parameter *Mn* and the relation between the value of *Mn* and the magnitude of **B**. Thus, we will examine a wide range of values for *Mn*, from 10^3 to 10^5 and discuss the effect of the magnetic field on the flow.

Blood also presents electrical conductivity σ which is hematocrit and temperature dependent (Papadopoulos and Tzirtzilakis, 2004). The electrical conductivity of stationary blood has been measured to be $\sigma = 0.7$ $(\Omega m)^{-1}$. A safe choice for the conductivity value is $\sigma = 0.8$ $(\Omega m)^{-1}$. According to Tzirtzilakis (2005), the additional term due to the Lorentz force would appear in Equation (9) and it would be:

$$-Mn_m H^2 u \quad \text{where } Mn_m = \frac{D^2 \sigma B_0^2}{\nu \rho}$$

Considering the aforementioned hypothetical case for flow under a magnetic field of $B = 0.5\,\mathrm{T}$, the corresponding dimensionless parameter Mn_m would be 8.8×10^{-3}. From our results it was found that, for this value of Mn_m and for the present magnetic field orientation, the term that arises in Equation (10) due to the Lorentz force is five orders of magnitude less than the gradient of the pressure in this same equation. Thus it can be neglected from our consideration.

Concerning the numerical results, Figure 4 shows streamlines of the flow in the lower part of the duct for $\eta < -0.25$, in the middle η-z plane for $\xi = 0$. In the background of the figure there are contours of the normalized axial velocity $w/\bar{w}$ and their levels are shown in the label at the right side of the plot. In this flow configuration the magnetic dipole is located at $z = 2$. The flow corresponds to $\mathrm{Re} = 150$ and $Mn = 7 \times 10^4$. It is observed that a hump is developed in the streamline due to the effect of the magnetic field. The contours show a retardation of the flow in the area above the dipole. The effect of the magnetic field on the flow is confined in the area close to the magnetic source. This fact is due to the nature of the dipole field ($B \sim 1/r^2$).

The formation of the secondary flow is shown in Figure 5. The plots show streamlines of the secondary velocities in the cross-sectional plane at several downstream locations. These plots are only qualitative and they are presented in order to help the understanding of the secondary flow development. The case shown corresponds to $\mathrm{Re} = 300$ and $Mn = 10^5$. The first plot (a) shows the secondary flow streamlines at an axial location far upstream from the dipole at $z - z_s = -0.590$. The plot shows a small movement of the fluid towards the upper side of the duct under the effect of the magnetic field. Plot (b) shows the flow just upstream from the dipole at $z - z_s = -0.027$, where the intensity of the upward movement is increased. Plot (c) corresponds to $z - z_s = 0$, which is exactly above the dipole. In the core of the duct there is a stream of fluid moving upwards, while from the walls there are two symmetric streams of fluid moving downwards. The rest of the plots (d)-(p) show the flow pattern at locations downstream from the dipole. It is observed that there is a downward flow that evolves into two counter-rotating vortices. These vortices fade away as the fluid moves downstream, away from the magnetic source.

Figure 6 shows the downstream variation of the axial pressure gradient for different values of Mn. The first plot corresponds to $\mathrm{Re} = 150$. Close to the inlet the value of the axial pressure gradient corresponds to the fully developed flow in straight pipes and it is $dp_a/dz = -4{,}800$. The magnetic field begins to affect the axial pressure gradient, and

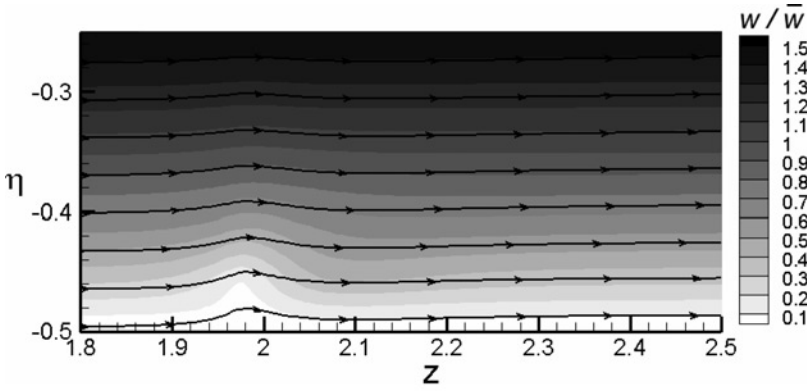

Notes: The magnetic dipole is located at $z = 2$

Figure 4.
Stream lines and normalized axial velocity contours in the lower part of the duct in the η-z plane, for $\xi = 0$ (middle plane) for $\mathrm{Re} = 150$ and $Mn = 7 \times 10^4$

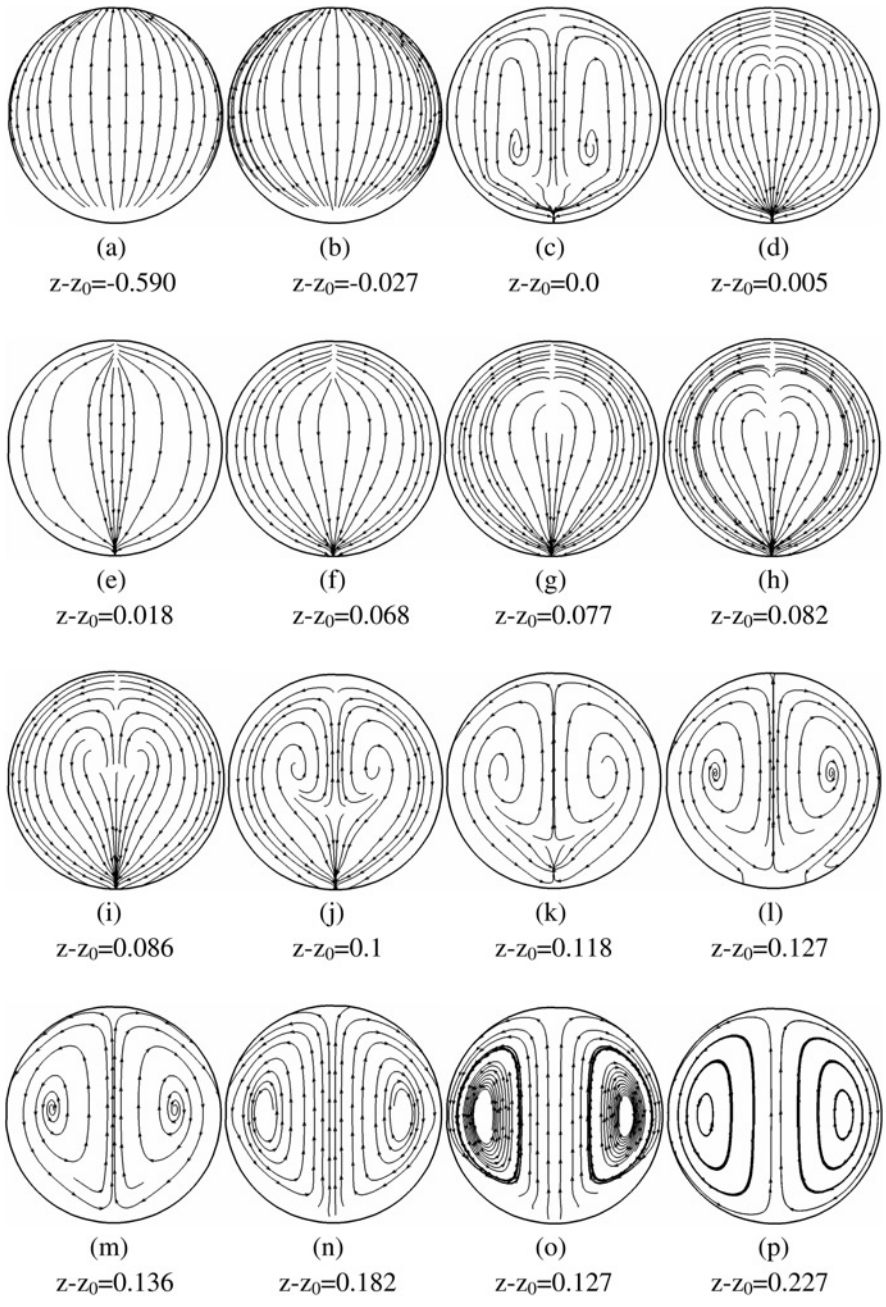

Notes: The streamlines are qualitative

Figure 5.
Streamlines in the ξ-η (transversal) plane at various downstream locations before and after the line dipole which is located at z_0 for Re $= 300$ and $Mn = 1 \times 10^5$

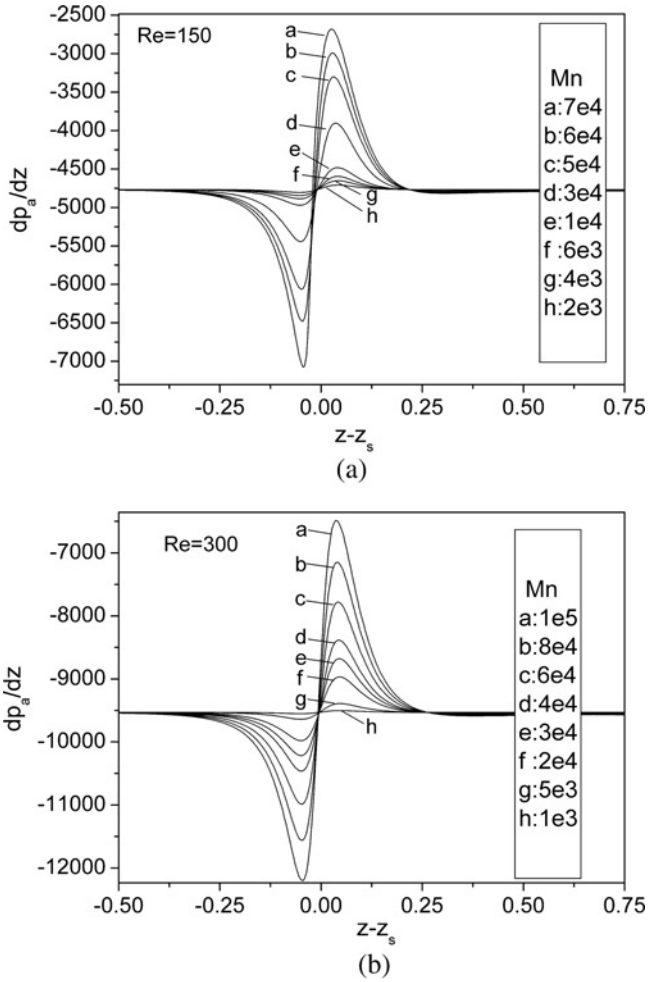

Notes: (a) Re = 150 and (b) Re = 300

Figure 6.
Variation of the axial pressure gradient in the axial direction for various values of *Mn*

consequently the behavior of the flow, at approximately $z - z_s = -0.25$. The axial pressure gradient presents a steep decrease as the flow approaches the source of the field at z_s. It reaches its lowest value at approximately $z - z_s = -0.005$, independently of the value of *Mn*. Then, dp_a/dz increases very rapidly in the region above the dipole, until $z - z_s = 0.023$ where it obtains its maximum value. Then it decreases again, since the effect of the magnetic field fades away as the fluid moves downstream. It is observed that the effect of the magnetic field is confined in the region $-0.25 < z - z_s < 0.25$.

This behavior of the axial pressure gradient conforms to the obstacle-like effect of the magnetic field on the flow. In the region before the dipole, the magnetic field effect virtually makes the flow passage narrower by repelling the magnetic fluid away from the dipole. Consequently, there is a stream with a steady mass flux passing through a constantly narrowed passage. This situation results in an increase of the pressure drop.

In the region above the magnetic source the gradient of H is reversed and the dipole attracts the magnetic fluid. This has the same effect as a sudden widening of the flow passage and consequently there is a sudden decrease of the pressure drop. In the final region the magnetic fluid attraction from the dipole apprehends the flow and the pressure drop increases again. However, the effect of the magnetic field gradually fades away and dp_a/dz returns eventually to its initial value.

The same conclusions are obtained from Figure 6b which depicts the axial variation of dp_a/dz for $\mathrm{Re} = 300$ and for various values of Mn. From the examination of the two plots of Figure 6 it is observed that the variation of the magnetic number Mn does not affect the range of the magnetic field effect. The limits of the field effect are 0.25 before and 0.25 after the location of the dipole and the locations of the maxima and minima of dp_a/dz curves remain unchanged and they do not depend on Mn. A similar observation can be made for the Reynolds number. The locations of the maxima and minima of the dp_a/dz curves as well as the limits of the magnetic field effect are the same for both $\mathrm{Re} = 150$ and 300.

From the two plots of Figure 6 it is also observed that the variation of dp_a/dz depends strongly on Mn. For low Mn of the order of 10^3 there is little variation of dp_a/dz, while for high Mn the variation of dp_a/dz reaches 50 per cent of the initial value. These facts are shown more clearly in the plots of Figure 7 that depict the maximum and minimum values of the downstream variation of dp_a/dz for $\mathrm{Re} = 150$ and 300. Each plot also includes two lines showing a linear variation of the maximum and minimum value of dp_a/dz with rates of 0.028 and -0.0195, respectively. It is observed that the variation of the maximum downstream value of dp_a/dz is very close to the linear behavior and it departs from it only for $Mn > 3 \times 10^4$. The variation of the minimum downstream value of dp_a/dz departs from linearity for $Mn > 10^4$. Thus, it is concluded that the linear approximation of the maximum and minimum value of dp_a/dz is valid for $Mn \leq 10^4$. It is also observed that the inclinations of the max and min curves are not affected by the Reynolds number. Thus, it is possible to predict the limiting values of the axial pressure gradient variation by knowing Re and Mn and consequently to estimate the friction losses via the friction factor product $f\mathrm{Re}$ of Equation (14). For the estimation of the maximum and minimum axial pressure gradient values we propose the following relations:

$$\begin{aligned} (dp_a/dz)_{\max} &= -32\mathrm{Re} + 0.028Mn \\ (dp_a/dz)_{\min} &= -32\mathrm{Re} - 0.0195Mn \end{aligned} \tag{16}$$

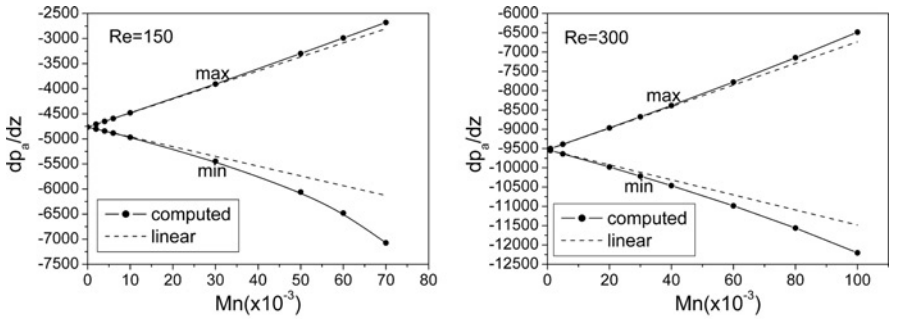

Figure 7.
Variation of the maximum and minimum values of the axial pressure gradient for various values of Mn

Notes: (a) Re = 150 and (b) Re = 300

The predictions of the relations deviate by less than 5 per cent from the computed results for $Mn \leq 10^4$ and $500 \geq \mathrm{Re} \geq 50$. For lower Re the deviation increases and in the case $\mathrm{Re} = 25$ and $Mn = 10^4$ the maximum discrepancy was 15 per cent.

The local effect of the magnetic field in the area above the dipole was investigated by the friction coefficient product $C_f\mathrm{Re}$ defined in Equation (14). As expected the variation of the mean value $C_f\mathrm{Re}$ is similar to that of the axial pressure gradient, since the two quantities are related (in straight duct flow without magnetic field they are related by the relation $C_f = f/4 = -(dp_a/dz)/2\mathrm{Re}^2$) (Incropera and De Witt, 1990). The friction coefficient decreases ahead of the line dipole, then increases very quickly in the area above the dipole and finally decreases again to reach its initial value. It was found that at the location $\xi = 0$, $\eta = -D/2$, which is the closest to the magnetic source and the field has maximum strength, there is a significant reduction of $C_f\mathrm{Re}$. The maximum reduction of $C_f\mathrm{Re}$ upstream of the dipole for various values of Mn at $\xi = 0$, $\eta = -D/2$ is shown in Table I. Table I also shows the maximum increase of $C_f\mathrm{Re}$ downstream from the dipole. The percentages of both the decrease and the increase of $C_f\mathrm{Re}$ are with respect to the flow in a straight duct without magnetic field where there is constant $C_f\mathrm{Re} = 16$. It is observed that the variation of $C_f\mathrm{Re}$ depends on Re. For the low velocity of $\mathrm{Re} = 150$ there is a reduction of the friction coefficient of approximately 8 per cent upstream from the dipole for $Mn = 10^4$, while for $Mn = 6 \times 10^4$ the reduction is more than 50 per cent. These changes are milder for the flow with $\mathrm{Re} = 300$, and for $Mn = 6 \times 10^4$ the reduction of $C_f\mathrm{Re}$ is approximately 16 per cent.

5. Conclusions

In the present study we investigated the biomagnetic fluid flow under the presence of a line dipole. The spatial limit of the field effect is confined close to the magnetic source due to the nature of the dipole field and it is not affected by the magnetic number Mn or by the Reynolds number Re. Concerning the friction factor of the flow, expressed by the pressure drop dp_a/dz, it is found that its limiting (max-min) values have a linear dependence from Mn and a relation is proposed for their prediction. Another observation made in the present study is that there is a significant decrease of the local friction coefficient $C_f\mathrm{Re}$ in the vicinity of the magnetic source. The decrease depends on the Reynolds number and Mn. For $\mathrm{Re} = 150$ and $Mn = 10^4$, which corresponds to $B = 0.5\,\mathrm{T}$, $C_f\mathrm{Re}$ is reduced by approximately 8 per cent. This information is useful for all kinds of applications that deal with blood flow in the presence of a magnetic field and designate the importance of taking into account the magnetic properties of blood when designing relevant equipment or disease treating methods.

Table I. Maximum reduction and increment of the friction coefficient $C_f\mathrm{Re}$ upstream and downstream of the dipole, respectively

	Re = 150			Re = 300	
Mn	Reduction of $C_f\mathrm{Re}$ (%)	Increment of $C_f\mathrm{Re}$ (%)	Mn	Reduction of $C_f\mathrm{Re}$ (%)	Increment of $C_f\mathrm{Re}$ (%)
2×10^3	1.7	0.6	2×10^3	0.3	0.1
1×10^4	7.8	3.6	1×10^4	5	1.8
6×10^4	54.1	20.8	6×10^4	15.7	5.4

Notes: $\xi = 0$, $\eta = -D/2$, for various values of Mn and $\mathrm{Re} = 150$, 300

References

Bovendeerd, P.H.M., van Steenhoven, A.A., van de Vosse, F.N. and Vossers, G. (1987), "Steady entry flow in curved pipe", *Journal of Fluid Mechanics*, Vol. 177, pp. 233-46.

Ganguly, R. and Puri, I.K. (2007), "Field-assisted self-assembly of superparamagnetic nanoparticles for biomedical MEMS and BioMEMS applications", *Advances in Applied Mechanics*, Vol. 41, pp. 293-335.

Ganguly, R., Gaind, A.P. and Puri, I.K. (2005a), "A strategy for the assembly of three dimensional mesoscopic structures using a ferrofluid", *Physics of Fluids*, Vol. 17 (057103).

Ganguly, R., Zellmer, B. and Puri, I.K. (2005b), "Field-induced self-assembled ferrofluid aggregation in pulsatile flow", *Physics of Fluids*, Vol. 17 (097104).

Ganguly, R., Gaind, A.P., Sen, S. and Puri, I.K. (2005c), "Analyzing ferrofluid transport for magnetic drug targeting", *Journal of Magnetism and Magnetic Materials*, Vol. 289, p. 331.

Haik, Y., Pai, V. and Cheng, C.-J. (1999), "Biomagnetic fluid dynamics", in Shyy, W. and Narayanan, R. (Eds), *Fluid Dynamics at Interfaces*, Cambridge University Press, Cambridge, pp. 439-52.

Haik, Y., Pai, V. and Cheng, C.-J. (2001), "Apparent viscosity of human blood in a high static magnetic field", *Journal of Magnetism and Magnetic Materials*, Vol. 225 Nos. 1/2, pp. 180-6.

Hatzikonstantinou, P.M. and Sakalis, V.D. (2004), "A numerical-variational procedure for laminar flow in curved square ducts", *International Journal of Numerical Methods in Fluids*, Vol. 45, pp. 1269-89.

Higashi, T., Ashida, N. and Takeuchi, T. (1997), "Orientation of blood cells in static magnetic field", *Physica B: Condensed Matter*, Vol. 237/238, pp. 616-20.

Higashi, T., Yamagishi, A., Takeuchi, T., Kawaguchi, N., Sagawa, S., Onishi, S. and Date, M. (1993), "Orientation of erythrocytes in a strong static magnetic field", *Blood*, Vol. 82, pp. 1328-34.

Incropera, F.P. and De Witt, D.P. (1990), *Fundamentals of Heat and Mass Transfer*, 3rd ed., Wiley & Sons, Singapore.

Kaminski, M.D. and Rosengart, A.J. (2005), "Detoxification of blood using injectable magnetic nanospheres: a conceptual technology description", *Journal of Magnetism and Magnetic Materials*, Vol. 293 No. 1, pp. 398-403.

Liu, J., Flores, G.A. and Sheng, R. (2001), "In-vitro investigation of blood embolization in cancer treatment using magnetorheological fluids", *Journal of Magnetism and Magnetic Materials*, Vol. 225 Nos. 1/2, pp. 209-17.

Mathieu, J.-B., Beaudoin, G. and Martel, S. (2006), "Method of propulsion of a ferromagnetic core in the cardiovascular system through magnetic gradients generated by an MRI system", *IEEE Transactions on Biomedical Engineering*, Vol. 53 No. 2, pp. 292-9.

Motta, M., Haik, Y., Gandhari, A. and Chen, C.J. (1998), "High magnetic field effects on human deoxygenated hemoglobin light absorption", *Bioelectrochemistry Bioenergetics*, Vol. 47, p. 297.

Mykhaylyk, O., Dudchenko, N. and Dudchenko, A. (2005), "Doxorubicin magnetic conjugate targeting upon intravenous injection into mice: high gradient magnetic field inhibits the clearance of nanoparticles from the blood", *Journal of Magnetism and Magnetic Materials*, Vol. 293 No. 1, pp. 473-82.

Papadopoulos, P.K. and Hatzikonstantinou, P.M. (2004), "Comparison of the CVP and the SIMPLE methods for solving internal incompressible flows", in Topping, B.H.V. and Mota Soares, C.A. (Eds), *Proceedings of the Fourth International Conference on Engineering Computational Technology*, Civil-Comp Press, Stirling, Paper 82.

Papadopoulos, P.K. and Tzirtzilakis, E.E. (2004), "Biomagnetic flow in a curved square duct under the influence of an applied magnetic field", *Physics of Fluids*, Vol. 16 No. 8, pp. 2952-62.

Papadopoulos, P.K., Vafeas, P. and Hatzikonstantinou, P.M. (2008), "Numerical study of a new model for the magnetohydrodynamic flow of micropolar magnetic fluids in straight square ducts", in Topping, B.H.V. and Mota Soares, C.A. (Eds), *Proceedings of the Sixth International Conference on Engineering Computational Technology*, Civil-Comp Press, Stirling, Paper 96.

Patankal, S.V. and Spalding, D.B. (1972), "A calculation procedure for heat, mass and momentum transfer in three-dimensional parabolic flows", *International Journal of Heat Mass Transfer*, Vol. 15, pp. 1787-806.

Roath, S. (1993), "Biological and biomedical aspects of magnetic fluid technology", *Journal of Magnetism and Magnetic Materials*, Vol. 122 Nos. 1/3, pp. 329-34.

Rosengart, A.J., Kaminski, M.D., Chen, H., Caviness, P.L., Ebner, A.D. and Ritter, J.A. (2005), "Magnetizable implants and functionalized magnetic carriers: a novel approach for noninvasive yet targeted drug delivery", *Journal of Magnetism and Magnetic Materials*, Vol. 293 No. 1, pp. 633-8.

Rotariu, O.V. and Strachan, J.C. (2005), "Modelling magnetic carrier particle targeting in the tumor microvasculature for cancer treatment", *Journal of Magnetism and Magnetic Materials*, Vol. 293 No. 1, pp. 639-46.

Ruuge, E.K. and Rusetski, A.N. (1993), "Magnetic fluids as drug carriers: targeted transport of drugs by a magnetic field", *Journal of Magnetism and Magnetic Materials*, Vol. 122 Nos 1-3, pp. 335-9.

Sakalis, V.D., Hatzikonstantinou, P.M. and Papadopoulos, P.K. (2005), "A numerical procedure for the laminar developed flow in a helical square duct", *ASME Journal of Fluids Engineering*, Vol. 127, pp. 136-48.

Sakhini, L. (2003), "Magnetic measurements on human erythrocytes: normal, beta thalassemia major, and sickle", *Journal of Applied Physics*, Vol. 93, p. 6721.

Shalygin, A.N., Norina, S.B. and Kondorsky, E.I. (1983), "Behaviour of erythrocytes in high gradient magnetic field", *Journal of Magnetism and Magnetic Materials*, Vol. 31 No. 2, pp. 555-6.

Takeuchi, T., Mizuno, T., Higashi, T., Yamagishi, A. and Date, M. (1995), "Orientation of red blood cells in high magnetic field", *Journal of Magnetism and Magnetic Materials*, Vol. 140 No. 2, pp. 1462-3.

Taylor, C.A. and Humphrey, J.D. (2009), "Open problems in computational vascular biomechanics: hemodynamics and arterial wall mechanics", *Computer Methods in Applied Mechanics and Engineering*, Vol. 198 Nos 45/6, pp. 3514-23.

Thomas, P.D. and Middlecoff, J.F. (1980), "Direct control of grid point distribution in meshes generated by elliptic equations", *AIAA Journal*, Vol. 18, pp. 652-6.

Thompson, J.F., Thames, F. and Mastin, C.J. (1974), "Automatic numerical generation of body-fitted curvilinear coordinate system for field containing any number of arbitrary two-dimensional bodies", *Computational Physics*, Vol. 15, pp. 299-319.

Tzirtzilakis, E.E. (2005), "A mathematical model for blood flow in magnetic field", *Physics of Fluids*, Vol. 17 No. 077103, 15pp.

Tzirtzilakis, E.E. and Loukopoulos, V.C. (2005), "Biofluid flow in a channel under the action of a uniform localized magnetic field", *Computational Mechanics*, Vol. 36, pp. 360-74.

Voltairas, P.A., Fotiadis, D.I. and Michalis, L.K. (2002), "Hydrodynamics of magnetic drug targeting", *Journal of Biomechanics*, Vol. 35 No. 6, pp. 813-21.

Corresponding author
Polycarpos K. Papadopoulos can be contacted at: p.papadopoulos@des.upatras.gr